

Influence of calcium and magnesium ions on CO₂ corrosion of carbon steel in oil and gas production systems - A review

H. Mansoori*, D. Young, B. Brown, M. Singer

Institute for Corrosion & Multiphase Technology, Department of Chemical & Biomolecular Engineering, Ohio University, Athens, OH, 45701, USA



ARTICLE INFO

Keywords:
CO₂ corrosion
Scale
Corrosion product
CaCO₃
Isostructurality
Mixed metal carbonates

ABSTRACT

Calcium and magnesium ions are major constituent species in produced brines associated with oil and gas production. Existing literature is often contradictory and unclear as to whether the presence of such ions accelerates or retards general corrosion. Furthermore, their influence on initiation and propagation of localized corrosion remains ambiguous. This review presents state-of-the-art knowledge concerning how Ca²⁺ and Mg²⁺ influence the CO₂ corrosion mechanism. In addition, a best way forward is proposed in order to bridge the existing literature gaps in studying the influence of these alkaline earth cations on CO₂ corrosion.

1. Introduction

Oil and gas production involves the transmission of large quantities of fluid – hydrocarbons, water, CO₂ (carbon dioxide), H₂S (hydrogen sulfide) gases – in carbon steel pipelines. In this environment, corrosion and scaling happen simultaneously (Mansoori et al., 2017). The aqueous phase, also called brine, is a by-product of almost every hydrocarbon production system, containing significant concentrations of dissolved cations such as Ca²⁺ (calcium ion) and Mg²⁺ (magnesium ion) as well as dominant Na⁺ (sodium ion) and Cl⁻ (chloride ion) (Oddo and Tomson, 1994), (Mansoori et al., 2013a). Depending on the conditions, scales in the form of CaCO₃ (calcium carbonate), MgCO₃ (magnesium carbonate) or a mixture of both can precipitate. These scales are different from other precipitates such as FeCO₃ (iron carbonate) and FeS (iron sulfide) where the constituent cation, Fe²⁺ (ferrous ion), comes from the corroding surface steel. In this manuscript, FeCO₃ and FeS are defined as a corrosion product since the constituent cation comes from the corrosion process, where CaCO₃ and MgCO₃ are defined as a scale since the constituent cation comes from the bulk solution. Distinct bodies of research have been conducted that separately address scaling and corrosion in the oil and gas industry. However, there is minimal information in the literature relating to situations where corrosion and scaling simultaneously occur, despite there being indications that heavy scaling may lead to localized attack and loss of facility integrity (Mansoori et al., 2017), (Salman et al., 2007). Consequently, there is a need to explore the potential relationships between scaling and encountered corrosion phenomena.

CO₂ corrosion and scaling processes are both highly dependent on

the gas composition and related water chemistry. Different brines with complex chemistries are encountered in oil and gas production environments. However, most laboratory corrosion studies have been performed only in various dilute NaCl (sodium chloride) electrolytes while, in reality, many other ions are present in the produced brine. Divalent cations that form various carbonate layers have the potential to play a major role in the corrosion behavior of mild steel, especially in downhole conditions of oil and gas wells at high temperature and high pressure. Among these cations, Ca²⁺ and Mg²⁺ are usually present at the highest concentration in reservoir fluids. Table 1 shows an example of these high ion concentrations from wells in Western Pennsylvania (Dresel and Rose, 2010). In terms of corrosion products, it is widely accepted that FeCO₃ can form a protective layer and plays a significant role in CO₂ corrosion of mild steel (Kermani and Morshed, 2003). The presence of Ca²⁺ and Mg²⁺ can change the composition of the corrosion product layer since their carbonate crystal structures, calcite (one of the mineral names for CaCO₃) and magnesite (the mineral name for MgCO₃), are isomorphous with siderite (the mineral name for FeCO₃) possessing a hexagonal unit cell (Chai and Navrotksy, 2015), (Zoltai and Stout, 1984). However, the effect of Ca²⁺/Mg²⁺-containing solutions on the properties of the FeCO₃ layer and subsequent effect on CO₂ corrosion mechanisms are insufficiently documented. Because of this lack of knowledge, current mechanistic models do not account for the presence of Ca²⁺ and Mg²⁺ in their corrosion predictions. In most corrosion prediction models, Ca²⁺ and Mg²⁺ are only considered regarding the ionic strength of the aqueous solution (Nordsveen et al., 2003). Therefore, it is critical to extend the capability of predictive models to bridge the gap in knowledge associated with the presence of

* Corresponding author.

E-mail address: hm419213@ohio.edu (H. Mansoori).

Table 1

Example of ion concentrations from an oilfield brine.

TDS (g/L)	Conductivity ($\mu\text{S}/\text{cm}$)	Na^+ (mg/L)	K^+ (mg/L)	Mg^{2+} (mg/L)	Ca^{2+} (mg/L)	Sr^{2+} (mg/L)	Ba^{2+} (mg/L)	Cl^- (mg/L)
213	190,000	56700	190	2520	18000	691	171	122000

Ca^{2+} and Mg^{2+} . The main goals of this paper are to review the relevant literature and knowledge about the effect of such ions on CO_2 corrosion mechanisms and to provide a pathway for conducting future studies on this topic based on the shortcomings in the existing scientific literature.

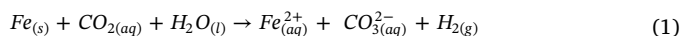
2. CO_2 corrosion and relevant corrosion products/scales

This section presents the fundamentals of CO_2 corrosion, including a brief review of the chemical and electrochemical reactions involved in CO_2 corrosion of mild steel. In addition, relevant corrosion products and scales encountered in CO_2 environments are discussed.

2.1. CO_2 corrosion of carbon steel in brief

Despite its vulnerability to CO_2 corrosion, carbon steel is the most used material for pipelines in the oil and gas industry, considering its cost-effectiveness. CO_2 corrosion, also known as sweet corrosion, is one of the major concerns in the oil and gas industry (Mansoori et al., 2013b), (Graver et al., 1984). CO_2 corrosion of carbon steel represents a phenomenon occurring when CO_2 dissolves in water and hydrates to become carbonic acid (H_2CO_3), which influences solution pH and provides cathodic species for reaction with the metal pipe surface. CO_2 corrosion has been investigated for more than four decades with the purpose of understanding its mechanisms and preventing or mitigating metal degradation. Modeling of the CO_2 corrosion mechanism began with de Waard and Milliams in 1975 (De Waard and Milliams, 1975) and continues to this day with fully mechanistic models (Institute for Corrosion and Multiphase Technology, 2014), (Nyborg, 2002).

CO_2 corrosion of carbon steel is an electrochemical process that involves the anodic dissolution of iron and the cathodic evolution of hydrogen. The overall reaction can be expressed as:



A number of chemical, electrochemical, and transport processes occur simultaneously in aqueous CO_2 corrosion of mild steel. The first step is the dissolution of gaseous carbon dioxide in water, as described in Equation (2). The second step is the hydration of aqueous CO_2 , which results in the formation of carbonic acid (H_2CO_3) as shown in Equation (3). This process is relatively slow and is often the rate-determining step in CO_2 corrosion (Kahyarian et al., 2017). The sequence of reactions associated with the presence of CO_2 in H_2O is as follows:

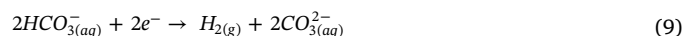
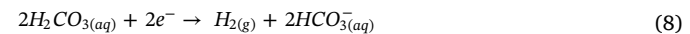


2.1.1. Electrochemistry of mild steel corrosion in CO_2 environments

The anodic reaction for oxidative iron dissolution is a key element in CO_2 corrosion, which takes place at the steel surface. The mechanism of iron dissolution in a CO_2 environment is complex and difficult to explain (Kahyarian et al., 2016). A number of multi-step mechanisms have been proposed by researchers for the anodic reaction of mild steel in CO_2 saturated aqueous media, which is outside the scope of this paper (Bockris et al., 1961; Dražić and Hao, 1982; Keddam, 2011). However, anodic dissolution of iron can be simply expressed by Equation (6):



the possible cathodic reactions in CO_2 environments in the absence of oxygen are listed below:



Past research mainly focused on the cathodic reactions to describe and model observed corrosion mechanisms (Nyborg, 2010). First, de Waard and Milliams proposed that the cathodic reaction in the form of Equation (8), the direct reduction of carbonic acid, would be dominant if the solution pH is greater than 4 (De Waard and Milliams, 1975). Ogundele and White also proposed that the direct reduction of bicarbonate ion, Equation (9), is important when the pH is higher than 5 (Ogundele and White, 1987). Nesic et al. later proposed that hydrogen ion reduction expressed by Equation (7) is the dominant reaction when the solution pH is less than 4 (Nesic et al., 1996). However, recent work by Tran et al., has cast some doubts on the previous understanding of the role of different cathodic reactions in CO_2 corrosion (Tran et al., 2015). Carbonic acid is a weak acid; it partially dissociates and serves as a hydrogen ion reservoir for the so-called “buffering effect” governing CO_2 corrosion. The authors demonstrated that for pH values below 6, at moderate partial pressures of CO_2 (less than 10 bar) and moderate temperatures (less than 80 °C), the dominant cathodic reaction is governed by hydrogen ion reduction, Equation (7), where the dissociation of carbonic acid, Equation (4), and dissociation of bicarbonate, Equation (5), provide H^+ through a buffering mechanism. This demonstrates that the mechanisms related to direct reduction reactions by carbonic acid and bicarbonate were negligible in their test conditions. To complete the list of cathodic reactions in sweet conditions, it can also be observed that the water reduction in Equation (10) plays an important role when the pH is higher than 6 for low partial pressures of CO_2 (Nesic et al., 1996).

2.1.2. FeCO_3

FeCO_3 is the main corrosion product from mild steel in CO_2 corrosion environments and has been proven to be protective under certain conditions (Nesic, 2007). FeCO_3 is considered as a corrosion product rather than scale since its constituent cations (Fe^{2+}) are derived from the corroding surface steel. The corrosion protection conferred by FeCO_3 is highly dependent on its growth rate, if the rate of corrosion is higher than FeCO_3 formation then it will not be protective; the ratio of precipitation rate to corrosion rate, labeled scaling tendency, can be used to qualify the layer protectiveness (Gao et al., 2011). FeCO_3 is formed from ferrous ions in solution that originates from corrosion and carbonate ions that are present due to CO_2 dissolution in water. Equation (11) describes precipitation (forward reaction) and dissolution (backward reaction) of FeCO_3 in aqueous solutions.



Precipitation occurs when the product of the ferrous ion and carbonate ion activities exceeds the solubility limit (K_{sp}) of FeCO_3 at equilibrium condition, Equation (12).

$$K_{sp,\text{FeCO}_3} = a_{\text{Fe}^{2+}} * a_{\text{CO}_3^{2-}} \quad (12)$$

where $a_{Fe^{2+}}$ is the ferrous ion activity (known as effective concentration), $a_{CO_3^{2-}}$ is the carbonate ion activity, and $K_{sp, FeCO_3}$ is the solubility product of $FeCO_3$ in the equilibrium condition. Ionic activity is related to concentration via Equation (13):

$$a_i = \gamma_i C_i \quad (13)$$

while γ_i is the appropriate activity coefficient, which can be calculated by an extended Debye-Hückel relationship, Equation (14), as proposed by Davies, for solutions with ionic strength up to 0.5 M (Davies, 1962). For complicated systems with higher ionic strength, the Debye-Hückel theory is no longer accurate. In such aqueous systems, advanced models such utilizing Pitzer equations can provide more realistic activity coefficients (Pitzer, 1991):

$$\log \gamma_i = -Az_i^2 \left(\frac{\sqrt{I}}{1 + \sqrt{I}} - 0.3*I \right) \quad (14)$$

the parameters associated with the above equations are:

a_i : activity of species i, (mol/L)

C_i : concentration of species i, (mol/L)

γ_i : activity coefficient of species i, (-)

$A = 1.82 \times 10^6 (\epsilon T)^{-3/2}$; $A \approx 0.5$ at 25°C (Stumm and Morgan, 2012)

ϵ : dielectric constant

T: solution temperature, (k)

z_i : charge of the species i, (-)

I: ionic strength of the solution, mol/L, described in Equation (16)

Sun et al., proposed Equation (15) for calculation of $K_{sp, FeCO_3}$ at different temperatures and ionic strengths (Sun et al., 2009):

$$\log K_{sp, FeCO_3} = -59.3498 - 0.041377*T_k - \frac{2.1963}{T_k} + 24.5724*\log(T_k) + 2.518*I^{0.5} - 0.657*I \quad (15)$$

where T_k is the temperature (in Kelvin) and I is the ionic strength (in mol/L), as determined by Equation (16):

$$I = \frac{1}{2} \sum_i c_i z_i^2 \quad (16)$$

where c_i is the concentration of each species in solution and z_i is the charge of the species.

Saturation degree (S) is a key parameter in scale or corrosion product forming situations. Equation (17) expresses the saturation degree with respect to $FeCO_3$:

$$S_{FeCO_3} = \frac{C_{Fe^{2+}} * C_{CO_3^{2-}}}{K_{sp, FeCO_3}} \quad (17)$$

where $C_{Fe^{2+}}$ and $C_{CO_3^{2-}}$ are ferrous ion and carbonate ion concentrations.

The $FeCO_3$ saturation degree greatly affects the corrosion behavior since it is the main driving force for $FeCO_3$ precipitation kinetics. When the saturation degree is less than unity (i.e., unsaturated condition), a higher corrosion rate is expected since a protective layer of $FeCO_3$ is not thermodynamically favored and may not be formed on the steel substrate. When the saturation degree is greater than unity (i.e., supersaturated solution), formation of $FeCO_3$ layer is expected. This can result in lowering of the uniform corrosion rate as the non-conductive $FeCO_3$ crystals can cover the metal surface and hinder mass transfer of relevant species for anodic and cathodic reactions (Nesic, 2007). When the saturation degree is close to unity, the rate of formation and dissolution of $FeCO_3$ can be similar, depending on the temperature.

2.2. $CaCO_3$ and $MgCO_3$

$CaCO_3$ and $MgCO_3$ are the most observed scales in oil production systems, and often exist as mixed carbonates. Precipitation happens

when their saturation degree is greater than unity. Similar to $FeCO_3$, the solubilities of $CaCO_3$ (calcite in this paper) and $MgCO_3$ decrease with increasing temperature. The available correlations for calculation of K_{sp} of $CaCO_3$ and $MgCO_3$ do not take into account the effect of ionic strength, unlike siderite, as shown in Equations (18) and (19), respectively (Plummer and Busenberg, 1982), (Bénédith et al., 2011). Therefore, for calculation of the saturation degree of these carbonates, the activity of ions should be considered rather than concentration. Equations (20) and (21) express how to calculate saturation degree for $CaCO_3$ and $MgCO_3$, accordingly.

$$\log K_{sp, CaCO_3} = -171.9065 - 0.077993*T_k + \frac{2839.319}{T_k} + 71.595*\log T_k \quad (18)$$

$$\log K_{sp, MgCO_3} = 7.267 - \frac{1476.604}{T_k} - 0.033918*T_k \quad (19)$$

$$S_{CaCO_3} = \frac{a_{Ca^{2+}} * a_{CO_3^{2-}}}{K_{sp, CaCO_3}} \quad (20)$$

$$S_{MgCO_3} = \frac{a_{Mg^{2+}} * a_{CO_3^{2-}}}{K_{sp, MgCO_3}} \quad (21)$$

$FeCO_3$ has the lowest solubility compared to $CaCO_3$ and $MgCO_3$. It means that in the same environmental condition, $FeCO_3$ reaches saturation prior to $CaCO_3$ and $MgCO_3$. Fig. 1 depicts how the solubility product constant (K_{sp}) of such carbonates change with temperature based on Equations (15), (18) and (19) (for consistency of the results, ionic strength is set to zero for Equation (15)). Earlier studies on $MgCO_3$ solubility have been conducted at specific temperatures and then the results were extrapolated to other conditions. This approach has led to discrepancies in the reported solubility for magnesite at different temperatures (Kittrick and Peryea, 1986), (Pokrovsky et al., 2009). Bénédith et al., have recently proposed Equation (19) for magnesite solubility which has been derived from extensive experimental solubility data conducted on synthetic magnesite at temperatures from 50 to 200 °C in 0.1 mol kg⁻¹ NaCl solutions with CO₂ partial pressure of 4–30 bars (Bénédith et al., 2011).

2.2.1. Isostructurality of calcite and magnesite with siderite

Being the main constituent of limestone, calcite is one of the most commonly observed minerals in sedimentary systems including oil reservoirs. Calcite crystallizes with a hexagonal unit cell as shown in Fig. 2.

Calcite and magnesite are isostructural with siderite meaning that they share the same crystal structure; note the trigonal carbonate anions packed between the calcium cations in Fig. 2. Each calcium is shielded by six oxygens from six different carbonates (Ca-O distance ca. 2.4 Å). Single unit cells of these minerals are shown in Fig. 3, Fig. 4, and Fig. 5. Each unit cell is shown perpendicular to their xy-plane. Note the

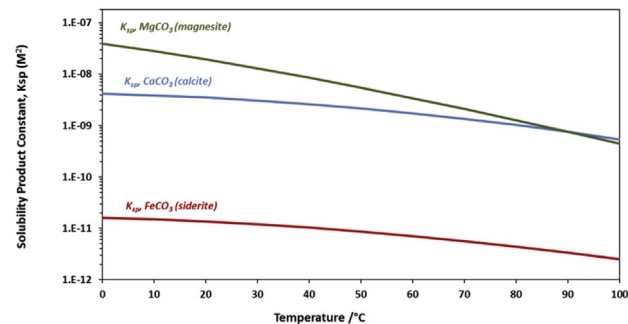


Fig. 1. Solubility products of siderite, calcite, and magnesite versus temperature.

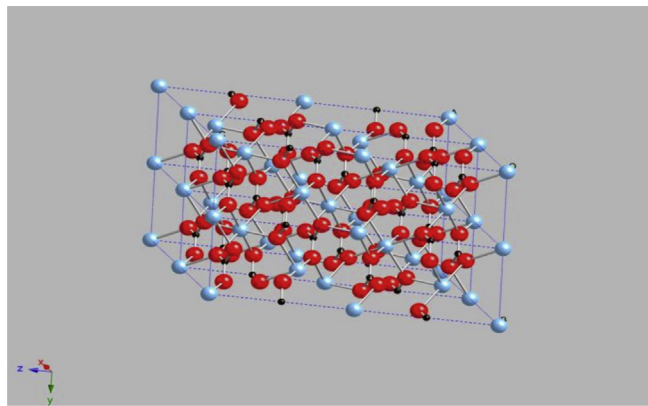


Fig. 2. Hexagonal crystal structure of calcite (CaCO_3 ; blue = Ca, red = O, black = C), four unit cells. (For interpretation of the references to colour in this figure legend, the reader is referred to the Web version of this article.)

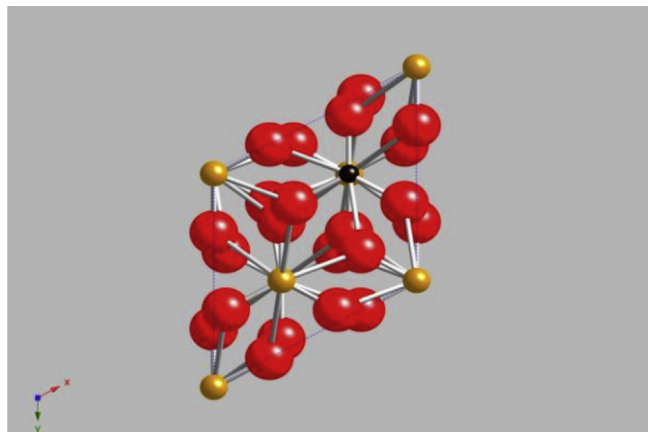


Fig. 3. Hexagonal single unit cell of siderite (FeCO_3 ; tan = Fe, red = O, black = C). (For interpretation of the references to colour in this figure legend, the reader is referred to the Web version of this article.)

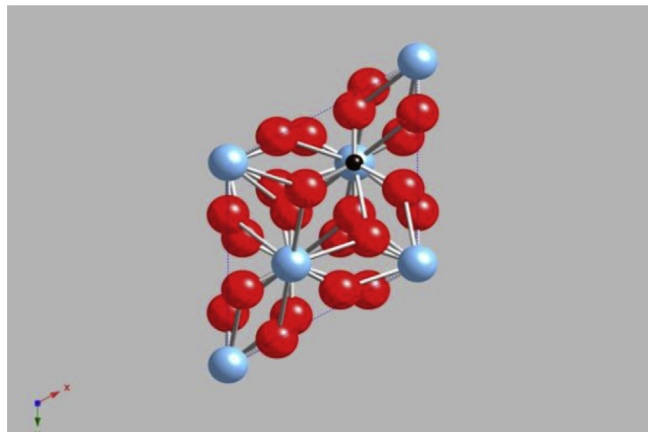


Fig. 4. Hexagonal single unit cell of calcite (CaCO_3 ; blue = Ca, red = O, black = C). (For interpretation of the references to colour in this figure legend, the reader is referred to the Web version of this article.)

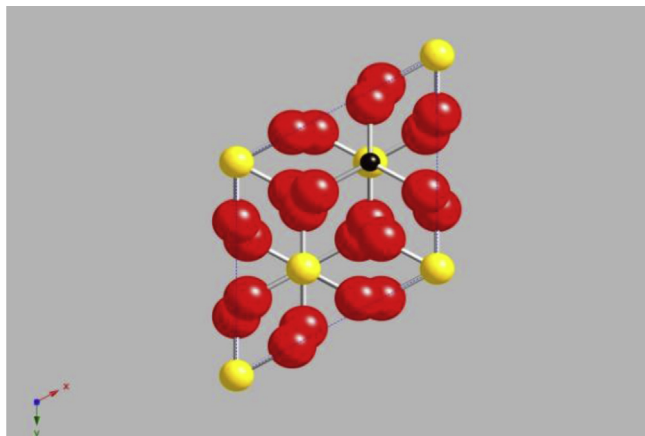


Fig. 5. Hexagonal single unit cell of magnesite (MgCO_3 ; yellow = Mg, red = O, black = C). (For interpretation of the references to colour in this figure legend, the reader is referred to the Web version of this article.)

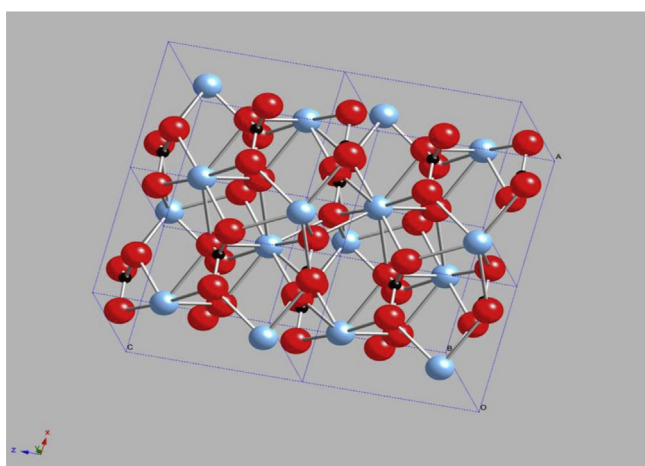


Fig. 6. Orthorhombic crystal structure of aragonite (CaCO_3 ; blue = Ca, red = O, black = C), four unit cells. (For interpretation of the references to colour in this figure legend, the reader is referred to the Web version of this article.)

(PbCO_3) (Chai and Navrotsky, 2015). The key difference of aragonite-type calcium carbonate from the calcite-type is that each calcium is shielded by nine oxygens from five different carbonate ions (Ca-O distance 2.4–2.6 Å). Consequently, the pseudo-octahedral geometry around each metal cation no longer applies. In addition, aragonite calcium carbonate is likely metastable, readily converting to calcite.

Magnesite, siderite, and calcite have the same unit cell type and similar cation radii and can co-exist in a solid solution (Chai and Navrotsky, 2015). Ca and Mg can replace Fe in the crystal structure of FeCO_3 and form a mixed substitutional solid solution. These substitutions have the potential to change the protective properties of FeCO_3 against further corrosion, as reported by various researchers (Zhao et al., 2005; Esmaeely et al., 2016; Ding et al., 2009). Table 2 shows key

Table 2
Key structural parameters for magnesite, siderite, and calcite.

Formula & Name	Cation Radius (Å)	Unit Cell Type	a (Å)	c (Å)	Density (g/cm ³)
MgCO_3 (magnesite)	0.72	hexagonal	4.59	14.87	3.01
FeCO_3 (siderite)	0.78	hexagonal	4.72	15.46	3.94
CaCO_3 (calcite)	1.00	hexagonal	4.99	17.04	2.71

structural parameters of these carbonates.

3. Literature review of the effect of Ca^{2+} and Mg^{2+} on CO_2 corrosion

Since a limited number of corrosion studies have been conducted using Ca^{2+} and Mg^{2+} , the corrosion mechanisms have not been methodically characterized. However, conducted experiments on this topic have, to a limited degree, elucidated CO_2 corrosion in the presence of these alkaline earth cations. A review of the available literature is provided below, which covers the main messages of each paper and their shortcomings. In section 4, a conclusive discussion on the literature review and future experimental path are presented.

Eriksrud and Sontvedt conducted one of the earliest studies to evaluate the effect of Ca^{2+} and Mg^{2+} along with other ions on CO_2 corrosion behavior of API 5L X52 specimens (Navabzadeh Esmaeely et al., 2013). Potentiodynamic sweep were conducted for three different brines with 0, 400 and 1200 ppm of Ca^{2+} at 20 °C, 1 bar partial pressure of CO_2 and over a pH range of 5.80–7.39. They concluded that formation of protective FeCO_3 layers enriched with Ca^{2+} resulted in a drop in corrosion rate of mild steel while the effect of Mg^{2+} on the general corrosion rate was reported to be negligible. One of the shortcomings of this research was that experimental durations were relatively short (2 days); therefore, possible phase transformation of the precipitated carbonates may not have been taken into account. CaCO_3 has three polymorphs, mineralogically named calcite, aragonite, and vaterite. Calcite is the most stable form of these CaCO_3 polymorphs (Zhong and Mucci, 1989). There have been reports in the literature that aragonite can transform to calcite after several days during corrosion experiments, resulting in possible change of mechanical properties (Navabzadeh Esmaeely et al., 2013).

Zhao et al., claimed that the corrosion rate decreased in the “short term” in the presence of Ca^{2+} and Mg^{2+} , but that there was no special difference for “long-term exposure” (Zhao et al., 2005). They postulated that the availability of Ca^{2+} and Mg^{2+} promoted the rapid formation of a protective layer in the short-term (before 72 h), which resulted in lower general corrosion rates. On the other hand, without Ca^{2+} and Mg^{2+} , a protective layer could form only with longer exposure time when Fe^{2+} concentration was sufficient for precipitation of corrosion products. They conducted experiments at 90 °C and CO_2 pressure of 25 bars, with 1000 ppm Mg^{2+} and 6000 ppm Ca^{2+} in solution. In addition to the corrosion behavior, the corrosion product morphology and composition were changed by the presence of Ca^{2+} and Mg^{2+} in the aqueous electrolyte. Inspection of the XRD data indicated that the most intense peak occurred at a position of less than 30° 2θ, which would be consistent with the larger Ca^{2+} being the major cation within the formed metal carbonate lattice. Peak broadening also seems to have occurred, consistent with inhomogeneity within the corrosion product-scale hybrid surface layers. The authors described the primary corrosion product as “amorphous $\text{Fe}(\text{Ca},\text{Mg})(\text{CO}_3)_2$ ” which was thicker than “crystalline FeCO_3 ”. Although pH plays a dominant role in corrosion and scaling processes, it was unreported in this work.

Gao et al., conducted autoclave corrosion experiments with a simulated brine from an oilfield to investigate the formation of surface layers at different test conditions and their effect on CO_2 corrosion of mild steel (Gao et al., 2008). The experimental conditions included different flow rates (0, 0.5 and 1 m/s) and partial pressures of CO_2 (0.1, 0.3 and 1 MPa) while the temperature was set to 65 °C, with 64 ppm Ca^{2+} , and 72 ppm Mg^{2+} . Based on energy dispersive X-ray spectroscopy (EDS) and X-ray diffraction (XRD) patterns, they suggested the formation of distinct phases of FeCO_3 , CaCO_3 , and MgCO_3 at 0.1 MPa p CO_2 , a solid solution of “ $(\text{Fe},\text{Ca},\text{Mg})\text{CO}_3$ ” at 0.3 MPa CO_2 partial pressure, and a solid solution of “ $(\text{Fe},\text{Ca})\text{CO}_3$ ” at 1 MPa CO_2 partial pressure. Fig. 7 shows an example of X-ray diffraction patterns of the surface layers formed on X65 carbon steel specimens at their quiescent condition. According to their work, at higher CO_2 pressure both general

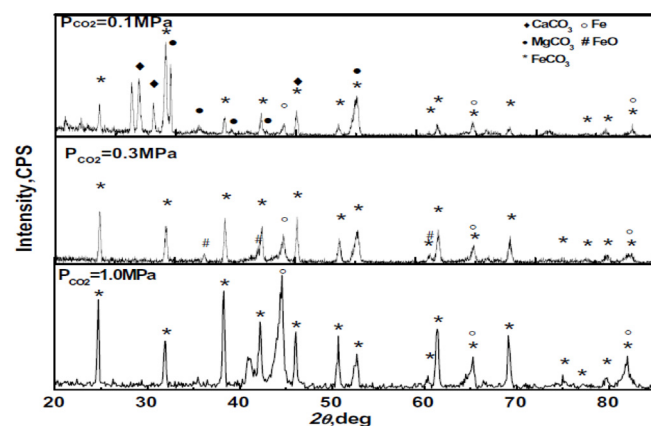


Fig. 7. X-ray diffraction patterns of the surface layers formed on X65 carbon steel specimens at various pCO_2 values, quiescent condition, 65 °C, 64 ppm Ca^{2+} , and 72 ppm Mg^{2+} (Gao et al., 2008).

and localized corrosion increased. However, in these experiments, the authors also did not report solution pH.

X. Jiang et al., conducted experiments in a glass cell at 57 °C, in the presence of 1000 ppm Ca^{2+} and at different concentrations of Cl^- to distinguish the effect of Cl^- and Ca^{2+} on pitting phenomena (Jiang et al., 2006). They carried out three experiments with different electrolytes, specifically 3 wt% NaCl, 3 wt% NaCl + 1.5 wt% CaCl_2 , and 4.6 wt% NaCl. Based on electrochemical impedance spectroscopy (EIS), they reported pitting initiation times were 70 h for the experiment with 3 wt % NaCl, 41 h for the 3 wt % NaCl + 1.5 wt% CaCl_2 electrolyte, and 23 h for 4.6% wt.% NaCl. Fig. 8 illustrates Nyquist plots over time for the experiment with 3 wt% NaCl + 1.5 wt% CaCl_2 , the specimens were made of API N80 steel. The diameter of the Nyquist semicircles increase over time up to 41 h. The authors attributed this behavior to the formation of protective layers on the steel surface and improvement of the protectiveness of the formed surface precipitates over time. However, the impedance noticeably decreased as the immersion time reached 49 h. According to Fig. 8, the impedance, again, gradually increased over the course of the experiment up to 96 h. The author related this phenomenon to propagation and “repassivation”, which the authors of this review interpret as pit death, associated with pitting corrosion. They also claimed that, while Cl^- caused pitting, the presence of Ca^{2+} postponed the pitting initiation time. While the authors did not propose a mechanism for pitting attack by Cl^- , their claim is in contrast with some other studies that suggest Cl^- has no effect on pitting corrosion of carbon steels (Jiang et al., 2013), (Fang et al., 2013). Another

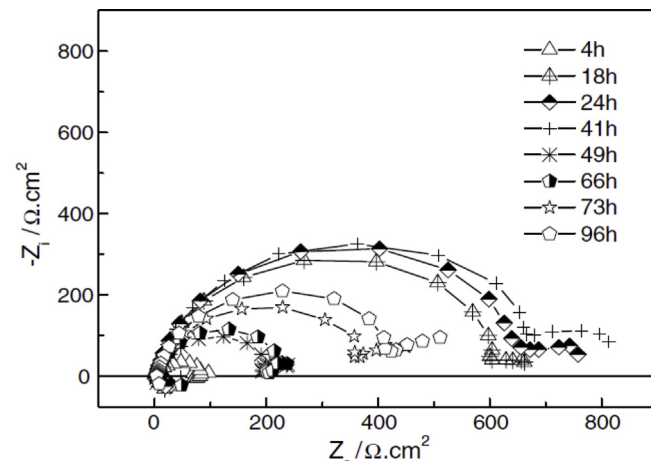


Fig. 8. Nyquist plots versus time for API CT5 N80 materials in 3 wt% NaCl + 1.5 wt% CaCl_2 electrolyte at 57 °C (Jiang et al., 2006).

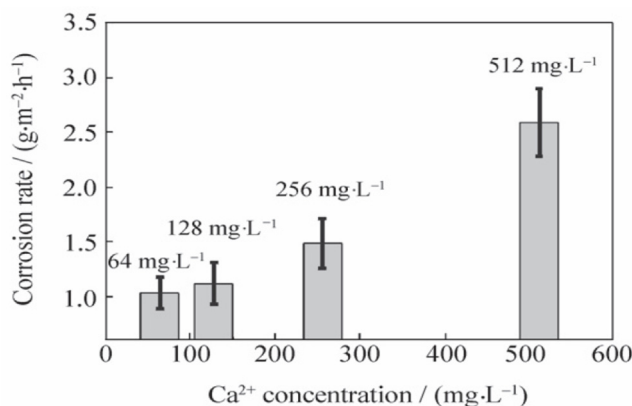
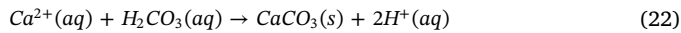


Fig. 9. Corrosion rate versus different concentrations of Ca²⁺ for X65 specimens at 75 °C and 10 bar pCO₂ after 10 days of exposure (Ding et al., 2009).

shortcoming of this work is that the authors did not measure the depth and width of pits; therefore, the magnitude of pitting rate was unquantified. In addition, the general corrosion rate for the different electrolytes was unreported.

Ding et al., conducted 10-day autoclave experiments with X65 specimens at 75 °C and 10 bar pCO₂ with up to 512 ppm of Ca²⁺ and 78 ppm Mg²⁺ to study the effect of Ca²⁺ concentration on corrosion behavior (Ding et al., 2009). They reported that the corrosion rate increased as the concentration of Ca²⁺ increased, as shown in Fig. 9. They also reported that the presence of calcium ions changed the corrosion product layer's crystal size. The authors concluded that the addition of Ca²⁺ forced the corrosion product layer crystals into morphological features that were “bigger” and “looser”; therefore, they did not act as a sufficiently protective barrier and, consequently, allowed corrosive species to more readily diffuse to the metal surface. They also showed XRD data, with shifted peaks from the FeCO₃ peak position with increasing Ca²⁺ concentration in the electrolyte. This shift is the result of the change in the unit cell of the corrosion products with the formation of mixed carbonate layers (Fe_{1-x}Ca_xCO₃). It is noteworthy that magnesium was undetected in their corrosion product. However, this is unsurprising as Mg²⁺ was present at a concentration close to its equilibrium concentration in relation to the solubility of MgCO₃ in water at the applied physicochemical conditions at the beginning of the experiment. The authors also reported formation of a bilayer on the steel surface. The concentration of calcium in the surface outer layer was higher than the inner layer, as confirmed by EDS and shown in Fig. 10.

Esmaily et al., studied the effect of Ca²⁺ on CO₂ corrosion at low and high concentrations of Ca²⁺ in 7-day glass cell experiments at 80°C and pCO₂ 0.53 bar (Navabzadeh Esmaily et al., 2013). They reported that for a low concentration of Ca²⁺ (up to 100 ppm) a protective layer formed and the corrosion rate decreased with time. However, for the electrolyte with a high initial concentration of Ca²⁺ (1000 and 10,000 ppm), the formed layers were non-protective and corrosion rate did not drop throughout the experiments; see Fig. 11. The authors also observed that the use of the electrolyte with 10,000 ppm Ca²⁺ led to severe pitting corrosion. In this research, the pH for the baseline test and the test with the presence of high concentration of Ca²⁺ were not identical. Upon adding such a high initial concentration of calcium ions (added as CaCl₂·2H₂O), massive precipitation of CaCO₃ acidified the electrolyte according to Equation (22). Therefore, it can be postulated that the increase in the corrosion rate was due to the lowered solution pH values rather than increased calcium ion concentration. pH behavior of electrolyte with different concentrations of Ca²⁺ is depicted in Fig. 12. It is worth noting that [Fe²⁺], [Ca²⁺], and pH were not kept constant over the course of experiments.



Tavares et al., conducted long-term (28 days) autoclave experiments to study the effect of CaCO₃ on the corrosion behavior of low carbon steel in high partial pressures of CO₂ (Tavares et al., 2015). The test electrolytes were saturated with CO₂ and NaCl at 80 °C, the pCO₂ was 15 Mpa. They designed two series of experiments, namely baseline and CaCO₃-saturated tests. The baseline test was carried out in the absence of CaCO₃. The CaCO₃-saturated test was conducted in the presence of a significant excess amount of solid CaCO₃ in the electrolyte (0.5 mol/kg; 10 times higher than its solubility limit), ensuring the solution was saturated with respect to CaCO₃ over the course of experiments. They claimed that general corrosion was predominant for both test series rather than pitting corrosion. Indeed, they reported a decline in the corrosion rate over time, as determined by mass loss. This behavior was observed for both tests, the authors related their findings to the formation of protective “corrosion scales”. Fig. 13 shows SEM images of “corrosion scale” morphologies after 72, 336, and 672 h of exposure to electrolytes with and without CaCO₃. For the CaCO₃-saturated solution, they reported formation of a carbonate solid solution with an average chemical composition of Fe_{0.79}Ca_{0.21}CO₃, concluded from EDS data. The corrosion product from the baseline condition was reported to be pure FeCO₃, with apparently larger crystal size compared to the “corrosion scales” formed in the presence of CaCO₃ (more evident after 72 and 336 h; see Fig. 13). It is interesting that even at such low initial pH values (2.71 and 4.7, respectively, for electrolyte without/with CaCO₃) carbonate layers precipitated. The authors did not measure or calculate pH at the end of their experiments. However, the solution water chemistry would have dramatically changed in the 1-liter autoclave over the course of experiments and resulted in final pH values significantly higher than for the initial conditions (Gao et al., 2017). Therefore, high pH and Fe²⁺ concentration (introduced to the solution from the corroding surface) has favored precipitation of FeCO₃ and Fe_xCa_{1-x}CO₃ over time in these experiments.

The authors also reported that the average corrosion rate in the presence of CaCO₃ was lower when compared to the solution without CaCO₃, as shown in Fig. 14. This was mainly due to a different initial pH of the two electrolytes rather than a direct effect of CaCO₃ on surface layer protectiveness against corrosion. Indeed, the corrosion rates after 336 and 672 h of exposure were almost identical for experiments with and without CaCO₃, meaning that water chemistry of the system was unchanged after 336 h. This work was one of the few corrosion studies conducted in electrolytes saturated with CaCO₃ and NaCl at a high partial pressure of CO₂. However, the main shortcoming of this research is that comparison of the two tests, with and without CaCO₃, may be problematic due to the considerable difference in the initial solution pH for each case; pH 4.7 for the solution with CaCO₃ and pH 2.71 for the solution without CaCO₃. However, this work showed that even in high concentrations of Ca²⁺ (around 2000 ppm; calculated from data provided by the authors), if the solution was saturated with respect to CaCO₃, a protective layer against further corrosion formed on the steel surface similar to the experiment in absence of CaCO₃. This is in contrast with other studies, as described earlier, reporting that with roughly similar Ca²⁺ concentrations, but different water chemistry conditions, a protective layer could not form (Ding et al., 2009), (Navabzadeh Esmaily et al., 2013). What can be concluded from this study is that the saturation degree of the carbonates is a critical parameter rather than calcium and magnesium ion concentration in evaluating the effect of Ca/Mg-containing aqueous solutions on CO₂ corrosion and solution pH measurements before and after the experiments are necessary to quantify this value.

4. Discussion and future experimental pathway

It is widely accepted that Ca²⁺ and Mg²⁺ do not directly participate in electrochemical reactions involved in CO₂ corrosion (George, 2003), but research related to these cations in solution have shown an influence on the corrosion rate. It is probable that a solid solution of

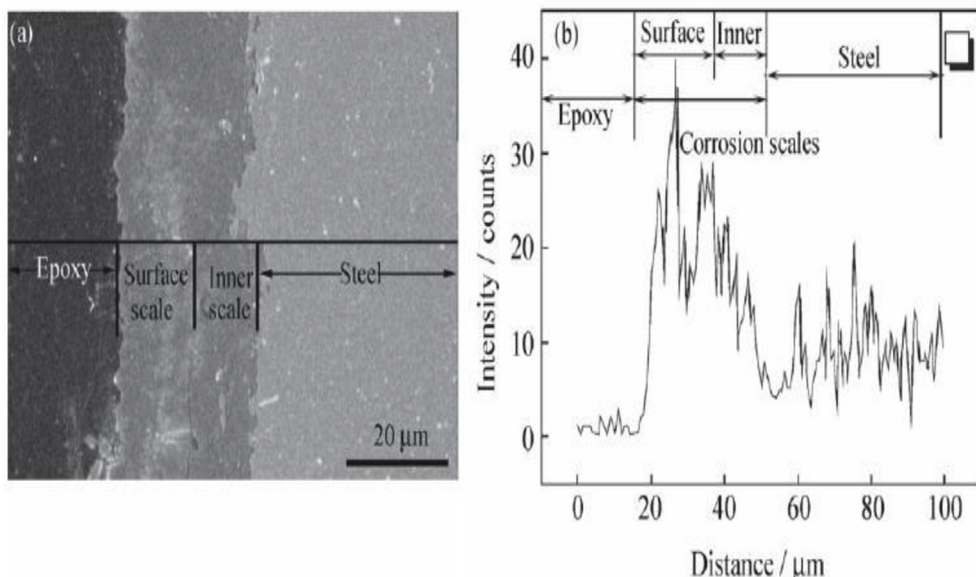


Fig. 10. Elemental analysis of the presence of calcium in the bilayers formed on the steel surface. Note the higher concentration of calcium in the outer layer (“surface scale”) compared to the inner layer (“inner scale”) when the test solution contained 512 ppm Ca^{2+} (Ding et al., 2009).

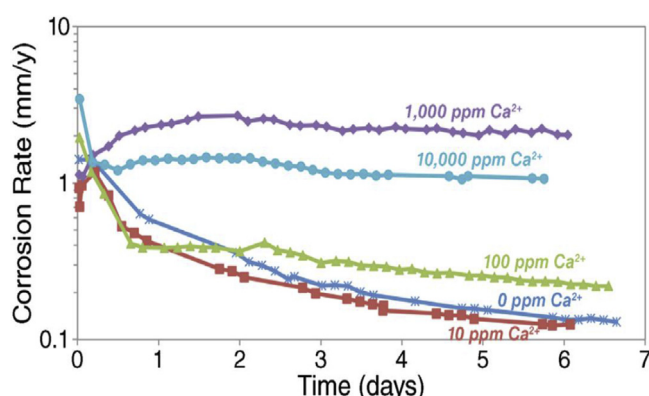


Fig. 11. Corrosion rate over time measured by LPR for different initial concentration of calcium ions at 80 °C, pCO_2 0.53 bar, 1wt % NaCl, and 10 ppm Fe^{2+} (Navabzadeh Esmaily et al., 2013).¹

$\text{Fe}_x\text{Ca}_y\text{Mg}_z\text{CO}_3$ (where $x + y + z = 1$) would form in CO_2 corrosion of mild steel in the presence of Fe^{2+} , Ca^{2+} , and Mg^{2+} dependent upon the available mole fraction of its constituents cations in solution. Heuristically speaking, a higher concentration of magnesium into a solid solution of $\text{Fe}_x\text{Ca}_y\text{Mg}_z\text{CO}_3$ would lead to an increase in solubility; this is because MgCO_3 has a higher solubility than FeCO_3 and CaCO_3 (Fig. 1). Therefore, the corrosion rate could dramatically increase with possible onset of localized attack when small changes in solution chemistry cause dissolution of Mg-bearing carbonates.

From a general literature review on this topic, one cannot conclusively describe the true effect of Ca^{2+} and Mg^{2+} on CO_2 corrosion for different water chemistries and conditions. There are studies claiming that the general corrosion rate is higher in the presence of calcium ions (Ding et al., 2009), (Navabzadeh Esmaily et al., 2013). Conversely, some researchers reported the exact opposite conclusions (Tavares et al., 2015), (Eriksrud and Sontvedt, 1984). In addition, there

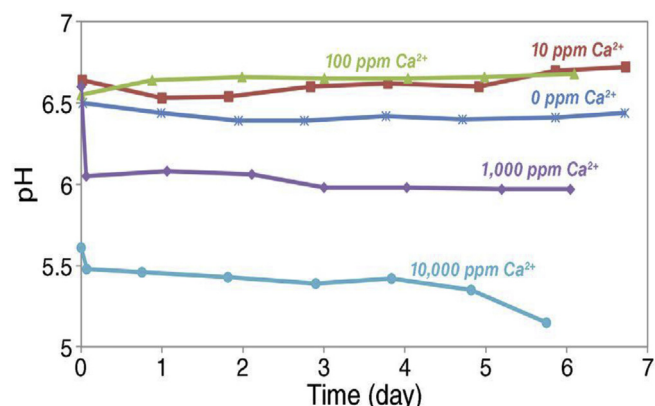


Fig. 12. Variation of pH over time for different concentrations of Ca^{2+} at 80 °C, pCO_2 0.53 bar, 1wt % NaCl, and 10 ppm Fe^{2+} (Navabzadeh Esmaily et al., 2013).¹ (note the difference in the electrolytes' pH caused by precipitation of CaCO_3 in high concentration of calcium ions).

are also experiments suggesting magnesium ions have no effect on CO_2 corrosion processes (Eriksrud and Sontvedt, 1984). Some researchers claimed that calcium ions initiate pitting corrosion attack (Navabzadeh Esmaily et al., 2013), while others stated that the presence of Ca^{2+} would postpone the pitting tendency on carbon steel (Jiang et al., 2006). These discrepancies about the true effect of Ca^{2+} and Mg^{2+} on CO_2 corrosion necessitate development of systematic and well-designed procedures in corrosion testing for understanding the relevant issues surrounding CO_2 corrosion in the presence of these ubiquitous alkaline earth cations.

One of the important parameters that has caused discrepancies in the open literature is the unknown and probably transient saturation degree of carbonates in the bulk solutions of autoclave, and glass cell, experiments. Saturation degree of the bulk solution is a more important parameter than the individual ion concentrations when studying the effect of Ca^{2+} and Mg^{2+} on corrosion mechanisms. Precipitation kinetics of carbonates is greatly influenced by the bulk saturation degree as the main driving force (Zhang et al., 2001), (Spanos and Koutsoukos, 1998). Most researchers have ignored this important environmental characteristic, solely relying on initial ion concentration as the core influencing parameter. Furthermore, the majority of available research

¹ Reproduced with permission from NACE International, Houston, TX. All rights reserved. Navabzadeh Esmaily, Saba, et al. Effect of calcium on the formation and protectiveness of iron carbonate layer in CO_2 corrosion, Corrosion, 69, 9, 2013. ©NACE International 1945.

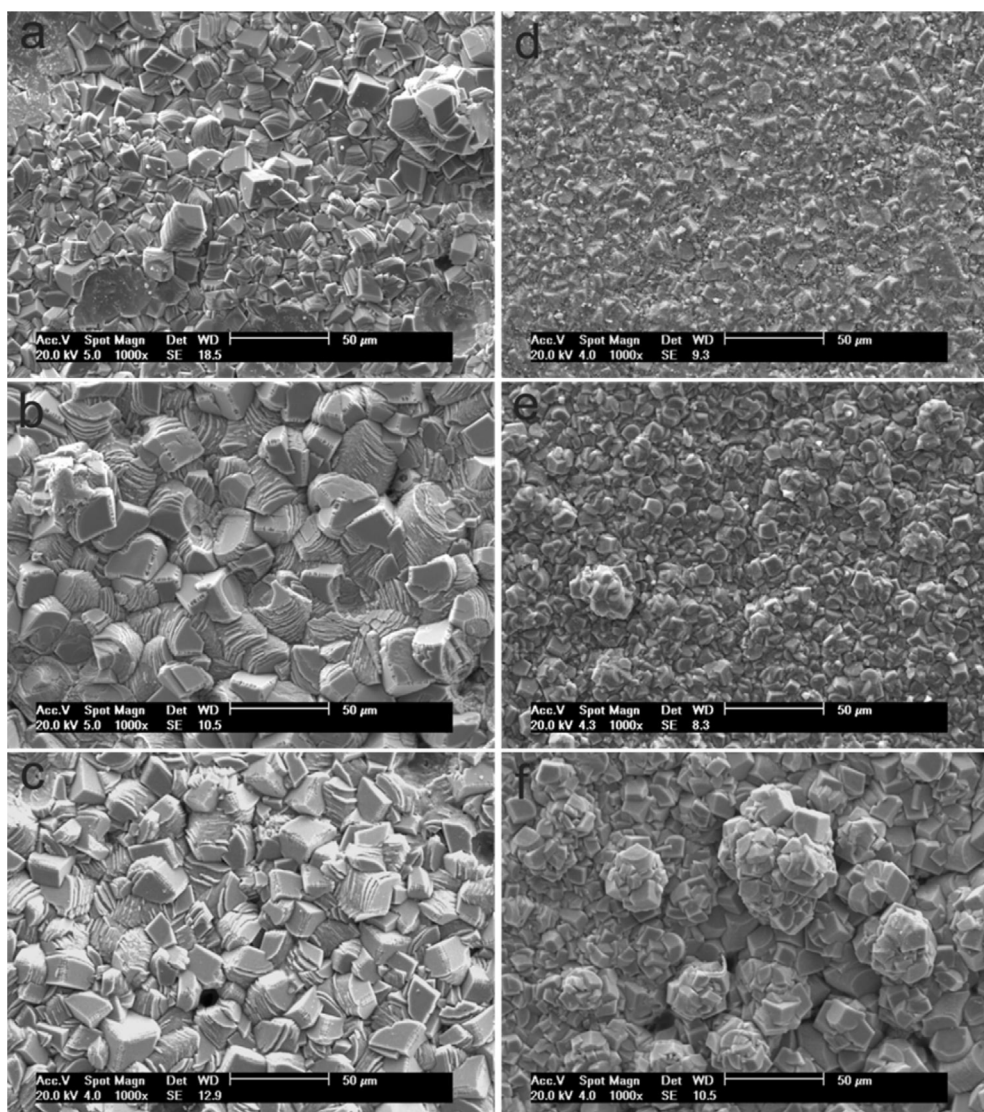


Fig. 13. SEM images of surface layers' morphology formed on low carbon steel after 72, 336, 672 h of exposure in CO_2 -saturated solutions (a, b, and c) without and (d, e, and f) with CaCO_3 (Tavares et al., 2015).

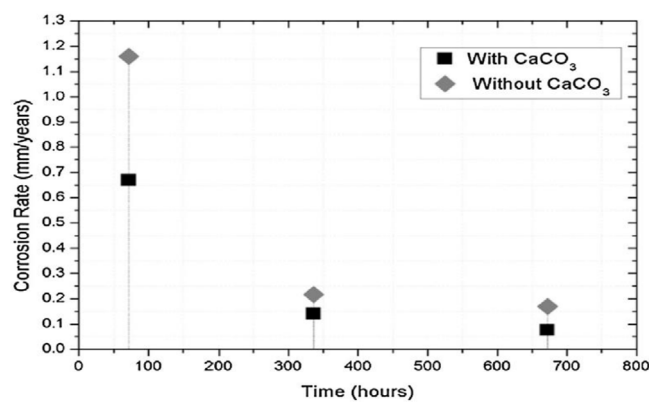


Fig. 14. Corrosion rate, by weight loss, versus exposure time for test electrolytes with and without CaCO_3 (Tavares et al., 2015).

on this topic has been conducted in conditions where the water chemistry of the systems was unstable (uncontrolled) and, in some cases, completely ignored (e.g., pH is unreported) (Zhao et al., 2005), (Ding et al., 2009). In addition, the flow characteristics of most of the

experimental setups were not appropriately studied and/or reported. Corrosion processes and formation of corrosion products/scales are influenced by the mass transfer of the relevant ions between the bulk solution and the metal surface (Nesic, 2012). These important parametric characteristics will significantly affect results, making experiments difficult to reproduce.

The current authors recommend that, for a precise study of the effect of Ca^{2+} and Mg^{2+} on CO_2 corrosion, experiments be conducted in relation to two distinct saturation scenarios with respect to CaCO_3 and MgCO_3 :

1. A non-scaling condition: when the solution is unsaturated, or at the saturation point, with respect to the CaCO_3 and MgCO_3 that can potentially form.
2. A scaling condition: when the solution is supersaturated with respect to CaCO_3 and MgCO_3 where it is expected that they will form.

It is worth mentioning that in corrosion studies the test solution, usually with small volume, will eventually be saturated with respect to FeCO_3 due to the corrosion process and production of Fe^{2+} . At such condition, precipitation of FeCO_3 , as the corrosion product, is expected.

In the non-scaling condition, the following fundamental question

needs to be answered:

- What is the effect of Ca^{2+} and Mg^{2+} on nucleation, growth, and precipitation of FeCO_3 ? There is report in the literature claiming the presence of calcium ions can hinder precipitation of FeCO_3 (Alsaiari et al., 2010). However, such claims need to be further investigated from the standpoint of corrosion.

Another relevant scenario is when the solution is supersaturated with respect to CaCO_3 and MgCO_3 . In such conditions, precipitation of carbonates from the bulk solution is expected. Therefore, carbonates, with distinct boundaries, can form affecting the homogeneity and porosity of the layers. The main questions in this condition are:

- Do such scales, without interference of ferrous ions, offer protectiveness against further corrosion? There is almost no data in the literature about the protective properties of pure CaCO_3 and MgCO_3 generated in aqueous CO_2 environments in studying the internal corrosion of pipelines.
- How does precipitation of CaCO_3 and MgCO_3 affect the formation of FeCO_3 ? An early postulate is that precipitation of such scales on the steel surface can provide more sites for heterogeneous nucleation and growth of the corrosion product, FeCO_3 , thus favoring its crystal growth. However, such postulates require verification through rigorous experimental design.

5. Conclusions

This review of literature data shows inconsistencies relating to the influence of Ca^{2+} and Mg^{2+} on CO_2 corrosion of mild steel. This is mainly due to undefined water chemistry and flow characteristics for most of the studied systems. Most of the previous work had focused on the initial concentrations of Ca^{2+} and Mg^{2+} as the core influencing parameter. This probably has resulted in completely different bulk saturation degrees with respect to the associated carbonates; saturation degree is the main driving force for precipitation of carbonates rather than the individual ions. Moreover, the water chemistry of the systems was uncontrolled and unknown in most studies, meaning that the initial and final test conditions were not the same. However, the available literature is indeed invaluable for spotlighting the mechanism of CO_2 corrosion in the presence of these alkaline earth cations. The literature unanimously agrees that Ca^{2+} and Mg^{2+} do not participate in electrochemical reactions at the steel surface and that a mixed metal carbonate can form in presence of Fe^{2+} , Ca^{2+} , and Mg^{2+} . Based on the literature review, the current authors have suggested two separate scenarios in conducting future experiments on this topic, namely in non-scaling and scaling conditions. Furthermore, for the sake of reproducibility of the results, the water chemistry of the system has to be defined and maintained, or at least documented, over the course of each experiment. Also, the flow characteristics of the system should be well-defined and reported since it affects the corrosion and scaling processes.

Acknowledgments

The authors would like to thank the following companies for their financial support during the writing of this review: Anadarko, Baker Hughes, BP, Chevron, CNOOC, ConocoPhillips, DNV GL, ExxonMobil, M-I SWACO (Schlumberger), Multi-Chem (Halliburton), Occidental Oil Company, PTT, Saudi Aramco, Shell Global Solutions, SINOPEC (China Petroleum), TransCanada, TOTAL, and Wood Group Kenny. The authors are also grateful to Dr. Bert Pots for discussions relating to preparation of this manuscript. All figures from other journals, reproduced herein, have been done so after securing permission from the original publishers.

References

- Alsaiari, H.A., Kan, A., Tomson, M., others, 2010. Effect of calcium and iron (II) ions on the precipitation of calcium carbonate and ferrous carbonate. *SPE J.* 15 (02), 294–300.
- Bénézeth, P., Saldi, G.D., Dandurand, J.L., Schott, J., Jun. 2011. Experimental determination of the solubility product of magnesite at 50 to 200 °C. *Chem. Geol.* 286 (1–2), 21–31.
- Boekris, J.O., Dražic, D., Despic, A.R., Aug. 1961. The electrode kinetics of the deposition and dissolution of iron. *Electrochim. Acta* 4 (2), 325–361.
- Chai, L., Navrotsky, A., 2015. Synthesis, characterization, and energetics of solid solution along the dolomite-ankerite join, and implications for the stability of ordered $\text{CaFe}(\text{CO}_3)_2$. *Am. Mineral.* 81 (9–10), 1141–1147.
- Davies, C.W., 1962. Ion association. Butterworths 37–53.
- De Waard, C., Williams, D.E., May 1975. Carbonic acid corrosion of steel. *Corrosion* 31 (5), 177–181.
- Ding, C., Gao, K., Chen, C., Dec. 2009. Effect of Ca^{2+} on CO_2 corrosion properties of X65 pipeline steel. *Int. J. Miner. Metall. Mater.* 16 (6), 661–666.
- Dražić, D.M., Hao, C.S., Oct. 1982. The anodic dissolution process on active iron in alkaline solutions. *Electrochim. Acta* 27 (10), 1409–1415.
- Dresel, P.E., Rose, A.W., 2010. Chemistry and Origin of Oil and Gas Well Brines in Western Pennsylvania. The Pennsylvania State University Open-File Report OFOG 10–01.0.
- Eriksrud, E., Sontvedt, T., 1984. Effect of flow on CO_2 corrosion rates in real and synthetic formation waters. *Proc. Symp. CO₂ Corros. Oil Gas Ind.* NACE 1, 20–38.
- Esmaeely, S.N., Young, D., Brown, B., Nesic, S., Nov. 2016. Effect of incorporation of calcium into iron carbonate protective layers in CO_2 corrosion of mild steel. *Corrosion* 73 (3), 238–246.
- Fang, H., Brown, B., Nesic, S., Mar. 2013. Sodium chloride concentration effects on general CO_2 corrosion mechanisms. *Corrosion* 69 (3), 297–302.
- Gao, M., Pang, X., Gao, K., Feb. 2011. The growth mechanism of CO_2 corrosion product films. *Corrosion Sci.* 53 (2), 557–568.
- Gao, S., Jin, P., Brown, B., Young, D., Nesic, S., Singer, M., Mar. 2017. Corrosion behavior of mild steel in sour environments at elevated temperatures. *Corrosion* 73 (8), 915–926.
- Gao, K., et al., Oct. 2008. Mechanical properties of CO_2 corrosion product scales and their relationship to corrosion rates. *Corrosion Sci.* 50 (10), 2796–2803.
- George, K., 2003. Electrochemical Investigation of Carbon Dioxide Corrosion of Mild Steel in the Presence of Acetic Acid. Ph.D. Dissertation. Ohio University.
- Graver, D.L., Newton, L.E., Hausler, R.H., 1984. *CO_2 Corrosion In Oil And Gas Production: Selected Papers, Abstracts, and References*. NACE International.
- Institute for Corrosion, Multiphase Technology, 2014. MULTICORP™. Ohio University.
- Jiang, X., Zheng, Y.G., Qu, D.R., Ke, W., Oct. 2006. Effect of calcium ions on pitting corrosion and inhibition performance in CO_2 corrosion of N80 steel. *Corrosion Sci.* 48 (10), 3091–3108.
- Jiang, X., Nesic, S., Kinsella, B., Brown, B., Young, D., Jan. 2013. Electrochemical investigation of the role of Cl^- on localized carbon dioxide corrosion behavior of mild steel. *Corrosion* 69 (1).
- Kahyarian, A., Singer, M., Nesic, S., Feb. 2016. Modeling of uniform CO_2 corrosion of mild steel in gas transportation systems: a review. *J. Nat. Gas Sci. Eng.* 29, 530–549.
- Kahyarian, A., Achour, M., Nesic, S., 2017. CO_2 corrosion of mild steel. In: Trends in Oil and Gas Corrosion Research and Technologies. Elsevier.
- Keddam, M., 2011. Anodic dissolution. In: *Corrosion Mechanisms in Theory and Practice*, Third. CRC Press, pp. 149–215.
- Kermani, M., Morshed, A., 2003. Carbon dioxide corrosion in oil and gas production-A compendium. *Corrosion* 59 (8), 659–683.
- Kittrick, J., Perrya, F., Feb. 1986. Determination of the gibbs free-energy of formation of magnesite by solubility methods. *Soil Sci. Soc. Am. J.* 50 (1), 243–247.
- Mansoori, H., Mowlavi, D., Esmaeilzadeh, F., Mohammadi, A.H., 2013a. Case study: production benefits from increasing C-values. *Oil Gas J.* 111 (6), 64–69.
- Mansoori, H., Mirzaee, R., Mohammadi, A.H., Esmaeilzadeh, F., 2013b. Acid washes, oxygen scavengers work against gas gathering failures. *Oil Gas J.* 111 (7), 106–111.
- Mansoori, H., Mirzaee, R., Esmaeilzadeh, F., Vojood, A., Soltan Dowranji, A., Dec. 2017. Pitting corrosion failure analysis of a wet gas pipeline. *Eng. Fail. Anal.* 82, 16–25.
- Navabzadeh Esmaeely, S., Choi, Y.-S., Young, D., Nesic, S., May 2013. Effect of calcium on the formation and protectiveness of iron carbonate layer in CO_2 corrosion. *Corrosion* 69 (9), 912–920.
- Nesic, S., Dec. 2007. Key issues related to modelling of internal corrosion of oil and gas pipelines—a review. *Corrosion Sci.* 49 (12), 4308–4338.
- Nesic, S., Jul. 2012. Effects of Multiphase flow on internal CO_2 corrosion of mild steel pipelines. *Energy Fuels* 26 (7), 4098–4111.
- Nesic, S., Postlethwaite, J., Olsen, S., 1996. An electrochemical model for prediction of corrosion of mild steel in aqueous carbon dioxide solutions. *Corrosion* 52 (4), 280–294.
- Nordsveen, M., Nesic, S., Nyborg, R., Stangeland, A., May 2003. A mechanistic model for carbon dioxide corrosion of mild steel in the presence of protective iron carbonate films—Part 1: theory and verification. *Corrosion* 59 (5), 443–456.
- Nyborg, R., 2002. Overview of CO_2 corrosion models for wells and pipelines. In: Presented at the CORROSION 2002.
- Nyborg, R., 2010. CO_2 corrosion models for oil and gas production systems. In: Presented at the NACE International.
- Ondo, J.E., Tomson, M.B., 1994. And others, “why scale forms in the oil field and methods to predict it. *SPE Prod. Facil.* 9 (01), 47–54.
- Ogundele, G., White, W., Nov. 1987. Observations on the influences of dissolved

- hydrocarbon gases and variable water chemistries on corrosion of an API L80 steel. *Corrosion* 43 (11), 665–673.
- Pitzer, K.S., 1991. Ion interaction approach: theory and data correlation. *Act. Coeff. Electrolyte Solut.* 75–154.
- Plummer, L.N., Busenberg, E., Jun. 1982. The solubilities of calcite, aragonite and vaterite in $\text{CO}_2\text{-H}_2\text{O}$ solutions between 0 and 90°C, and an evaluation of the aqueous model for the system $\text{CaCO}_3\text{-CO}_2\text{-H}_2\text{O}$. *Geochem. Cosmochim. Acta* 46 (6), 1011–1040.
- Pokrovsky, O.S., Golubev, S.V., Schott, J., Castillo, A., Jul. 2009. Calcite, dolomite and magnesite dissolution kinetics in aqueous solutions at acid to circumneutral pH, 25 to 150°C and 1 to 55 atm p CO_2 : new constraints on CO_2 sequestration in sedimentary basins. *Chem. Geol.* 265 (1–2), 20–32.
- Salman, M., Qabazard, H., Moshfeghian, M., Jan. 2007. Water scaling case studies in a kuwaiti oil field. *J. Petrol. Sci. Eng.* 55 (1), 48–55.
- Spanos, N., Koutsoukos, P.G., 1998. Kinetics of precipitation of calcium carbonate in alkaline pH at constant supersaturation. Spontaneous and seeded growth. *J. Phys. Chem. B* 102 (34), 6679–6684.
- Stumm, W., Morgan, J.J., 2012. *Aquatic Chemistry: Chemical Equilibria and Rates in Natural Waters*. John Wiley & Sons.
- Sun, W., Nesic, S., Woollam, R.C., 2009. The effect of temperature and ionic strength on iron carbonate (FeCO_3) solubility limit. *Corrosion Sci.* 51 (6), 1273–1276.
- Tavares, L.M., da Costa, E.M., Andrade, J. J. de O., Hubler, R., Huet, B., Dec. 2015. Effect of calcium carbonate on low carbon steel corrosion behavior in saline CO_2 high pressure environments. *Appl. Surf. Sci.* 359, 143–152.
- Tran, T., Brown, B., Nesic, S., 2015. Corrosion of mild steel in an aqueous CO_2 environment—basic electrochemical mechanisms revisited. In: Presented at the NACE Corrosion Conference.
- Zhang, Y., Shaw, H., Farquhar, R., Dawe, R., Apr. 2001. The kinetics of carbonate scaling—application for the prediction of downhole carbonate scaling. *J. Petrol. Sci. Eng.* 29 (2), 85–95.
- Zhao, G.X., Jian-Ping, L., Shi-Ming, H., Xiang-Hong, L.U., 2005. Effect of Ca^{2+} and Mg^{2+} on CO_2 corrosion behavior of tube steel. *J. Iron Steel Res. Int.* 12 (1), 38–42.
- Zhong, S., Mucci, A., Dec. 1989. Calcite and aragonite precipitation from seawater solutions of various salinities: precipitation rates and overgrowth compositions. *Chem. Geol.* 78 (3), 283–299.
- Zoltai, T., Stout, J.H., 1984. *Mineralogy: Concepts and Principles*. Burgess Publishing Company.